Micro Computed Tomography Based Quantification of Pore Size in Electron Beam Melted Titanium Biomaterials

SJ Tredinnick* JG Chase **

**NZi3 National ICT Innovation Institute, University of Canterbury, Christchurch, New Zealand (e-mail: seamus.tredinnick@pg.canterbury.ac.nz*
*** Department of Mechanical Engineering, University of Canterbury, Christchurch, New Zealand (e-mail: Geoff.chase@canterbury.ac.nz)*

Abstract: This paper presents a new method for the quantification of pore size of scaffold biomaterials from micro computed tomography (μCT). A two dimensional implementation of a spherical pore approximation model and a novel pore quantification algorithm have been applied to actual and phantom μCT reconstructions and the accurate measurement of pore size has been demonstrated. This paper describes the circular pore model used for the two dimensional analysis, a spherical pore model for three dimensional analysis, the algorithm for quantifying pore size, and the mechanics of the algorithm for both the 2-D and 3-D implementations.

Keywords: algorithms, biomedical systems, 3-D metallic constructs, metallic bone scaffolds, bone tissue engineering

1. INTRODUCTION

The Electron Beam Melting (EBM) of titanium to produce bone interfacing orthopaedic biomaterials is now in common use. These EBM titanium scaffolds are typically highly interconnected, ordered structures with large macro sized pores well in excess of traditional pore sizes such as those investigated by Marin (2010). Many of these titanium scaffolds have demonstrated excellent osseointegration properties as summarized by Alvarez and Nakajima (2009). With the advancement of scaffold architecture moving away from random and orthogonal lattices and towards bone mimicking morphology (trabecular structure) and incorporating aesthetic driven design the quantification of pore size has become more challenging. Significant work has been performed relating pore size to bone in-growth for orthopaedic biomaterials and so it is vital to the advancement of scaffold biomaterials that this metric be included in any design or analysis. There are limits of pore size above which vascularization of bone in-growth can occur and ranges of pore size that are more favourable to bone in-growth for specific pore architectures (Karageorgiou, 2005). This information can be easily incorporated in to scaffold design if the pore size of the scaffold can be readily determined.

The application of micro computed tomography (μCT) for pore quantification gives the capability to produce volumetric reconstructions in high resolution; typically 1-50μm per voxel. μCT scanning is non-destructive and can be performed on complete products to give insight to the final product structure in a production setting. Additionally, μCT can be used for bone in-growth, apposition, and quality quantification in-vitro, in-vivo, and ex-vivo (Jones, 2004). However, determining the pore characteristics of complex morphologies from a μCT scan can require a great deal of user input as traditional approaches have required the user identification of individual pores and landmarks from which to take measurements.

The algorithm presented takes an approach that can differentiate a pore from the surrounding interconnect region, approximate the pore diameter and do so in a scalable and automated environment to enable statistically relevant quantification to be performed in an automated fashion. The basis of the method presented is a spherical pore model which aims to simplify complex pore architecture and provide a comparative metric that can be used with many differing scaffold morphologies.

2. METHODS

2.1 Pore Model

For any interconnected scaffold structure the strut arrangement will constrain a porous region. Although the arrangement of the struts may be complex, for most strut arrangements the porosity can be adequately described as a collection of pores and interconnecting boundaries. With a spherical pore approximation model the individual pores constrained by a series of struts are modelled as the largest circumscribed spherical volume with the diameter of the sphere indicating the diameter of the pore. All internal fully constrained regions of a scaffold are described in this way. Where spherical pores intersect one and other the boundary between the adjacent pores is defined to be the interconnect region.

When dealing with highly interconnected structures, such as in (Fig. 1), there is often little differentiation between

adjacent pores. With a spherical pore approximation model pores are identified with a hierarchical approach where larger pores are determined before smaller pores. This approach ensures that an accurate indication of true pore size is achieved and that interconnecting regions are not falsely determined to be small pores.

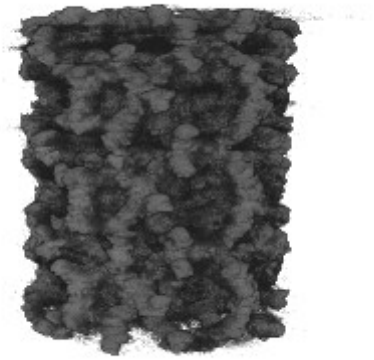

Fig. 1. A three dimensional μCT reconstruction of a complex scaffold manufactured by EBM. The scaffold is 5mm in diameter and 6mm in length.

2.2 Algorithm Overview

The constraint of a pore is achieved by a series of contact points. In the simple case when dealing with two dimensional slice data a circular pore can be fully defined by three contact points. When a three dimensional volumetric reconstruction is used a spherical pore is fully defined by four contact points.

Of importance to the accuracy of the pore approximation is the maximization of the pore size within the constraints of the scaffold. When dealing with complex structures the best approach is an iterative method that allows the incremental search from an initiation site to a local maximum in pore diameter while allowing the pore centre to shift as necessary to achieve this. The iterative migration of the pore centre is in a direction that allows the greatest expansion of the pore in a given iteration.

At each step of the search for a local maximum of pore diameter the contact points of a pore are re-established by expanding the pore to meet the closest contact points and where a new contact point is made a substitution of contact points occurs. If the pore is not fully constrained the pore is migrated to a new location. When a local maximum in pore diameter has been found the change in pore diameter will remain constant for all subsequent iterations and the search is complete.

As this process is repeated over many pore initiation sites all local maxima of pore diameters are found within the constraints of a scaffold and as such the sizes and locations of the pores of a scaffold are described.

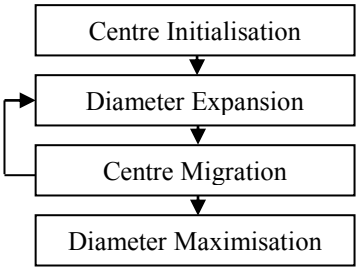

Fig. 2. A schematic diagram of the pore quantification algorithm for an individual pore.

2.3 Algorithm Mechanics

2.3.1 Determining the solution space and its boundaries

The solution space where the algorithm may look for pores is the inverse space of the struts comprising a scaffold and may be bounded externally by an artificial boarder. The boundaries of this solution space are the surfaces of the struts within a scaffold and are potential contact point locations.

2.3.2 Selecting suitable initiation sites

To ensure all pores within a scaffold are identified, suitable initiation sites for the search of pores must be selected. As pore centres will lie in regions of the solution space far away from the boundary these regions should be preferentially chosen for initiation sites. Pore initiation sites should be hierarchically chosen to favour sites farther from the boundary than those close to the boundary. As subsequent pores are found the regions of the solution space occupied by pores already quantified should be excluded from the search process.

2.3.3 Defining a pore in two dimensions

In the 2D regime a pore can be quantified as the largest possible circumcircle to fit within an area of interest. The circumcircle is fully defined by three contact points and a geometric construction of the circumcircle is given by Pedoe (1995).

2.3.4 Migration of a pore during a search in two dimensions

To determine the size of a pore contained within a region of the scaffold the pore is first initiated in an arbitrary location then expanded radially to fill the pore site. During this process the pore centre may migrate to enable the local maximum in pore diameter to be found. In 2D this migration is determined in the following ways: where there is one contact point the direction of the migration is opposite to the direction of the ray extending to that contact point (Fig. 3); where there are two contact points the direction of the migration is opposite to the bisector of the angle between the two rays extending to the two contact points (Fig. 4). Where there are three contact points the circular pore is fully defined (Fig. 5).

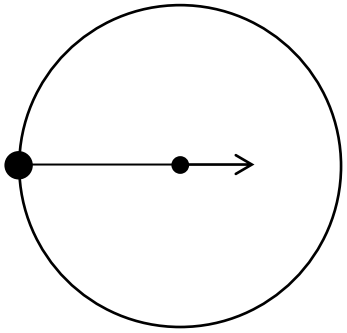

Fig. 3. Migration direction for one contact point.

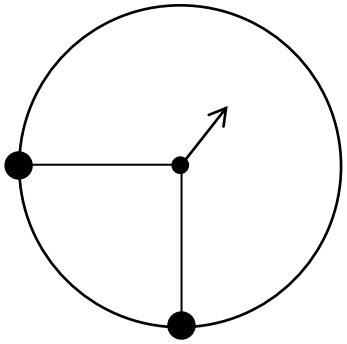

Fig. 4. Migration direction for two contact points.

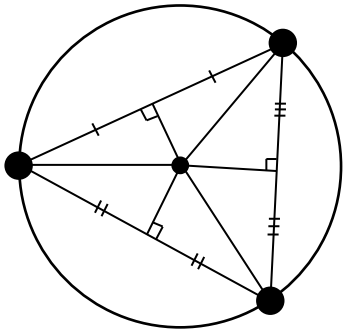

Fig. 5. The circle is fully defined by three contact points.

2.3.5 Defining a pore in three dimensions

In the 3D regime a pore can be quantified as the largest possible circumsphere to fit within a volume of interest. The circumsphere is fully defined by four contact points and can be constructed with an extension of the geometric construction of the circumcircle.

2.3.6 Migration of a pore during a search in three dimensions

In 3D the pore centre migration is determined in a similar fashion as for 2D with an extension of this method in the case of having 3 contact points. For three contact points the direction of migration is the opposite to the trisector of the angles made between rays extending to the three contact points (an extension of the case shown in Fig. 4). Where there are four contact points the spherical pore is fully defined.

2.3.7 Determining the interconnecting boundaries of pores

Where there are two adjacent pores the minimum throat diameter of the interconnecting region between them is considered to be the interconnecting boundary. For a 2D reconstruction this boundary is a linear and for a 3D reconstruction this boundary is planar.

3. RESULTS

3.1 A simple pore in two dimensions from phantom data

To demonstrate the pore model and ensure the algorithm can accurately determine pore size a simple phantom was evaluated. A phantom consisting of a simple cubic structure with two dimensional slices oriented at 0° was used (Fig. 6). The two dimensional image produced had a canvas size of 100x100 pixels (px). Circular struts (each 10px in diameter) were placed at the corners of the canvas. The algorithm was applied to this phantom and the pore size was measured.

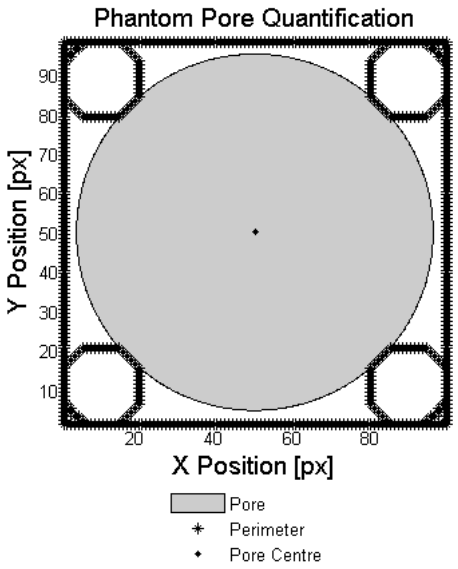

Fig. 6. Two dimensional pore quantification of a pore in a simple cubic scaffold phantom.

Table 1. Phantom pore quantification

Actual Pore Diameter [px]	Measured Pore Diameter [px]	Error
90.5	90.47	2.7%

The pore was found to be 90.47 pixels in diameter which is within 2.7% error of the original dimensions of the phantom pore indicating that the algorithm can accurately determine pore size.

3.2 A simple pore in two dimensions from µCT data

Following the validation of the algorithm on phantom data the pore size of a µCT slice of an EBM scaffold was analysed. Analysing actual data is significantly more challenging that simulated data due to significant levels of noise both in the form of CT artefact and topographical roughness of the scaffold. To deal with CT artefact the image was filtered to reduce noise prior to analysis. The robust application of the pore migration techniques (2.3.2) ensured that the local maximum in pore diameter was found irrespective of topological roughness.

A two dimensional slice (Fig. 8) of unit cell of a simple scaffold (Fig. 7) was chosen and the pore size of the bounded pore was quantified.

A comparison was made showing the difference in pore size reported with the spherical pore approximation model to a traditional µCT technique, such as that shown in by Ho, S.T. (2006), which involves measurement of a pore between scaffold struts at the surface of a scaffold. Fig. 10 shows the pore size measurement for a simple scaffold that would be reported using this technique.

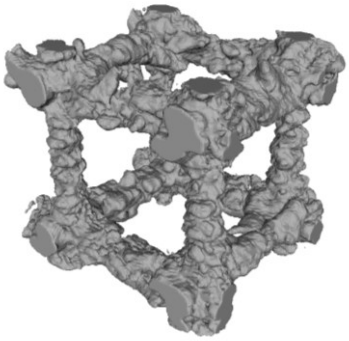

Fig. 7. A three dimensional µCT reconstruction of a unit cell of a simple scaffold manufactured by EBM.

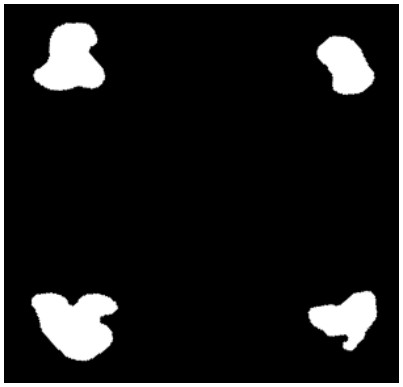

Fig. 8. A filtered and thresholded two dimensional slice reconstructed from a µCT scan of the unit cell of the simple EBM scaffold shown in Fig. 7.

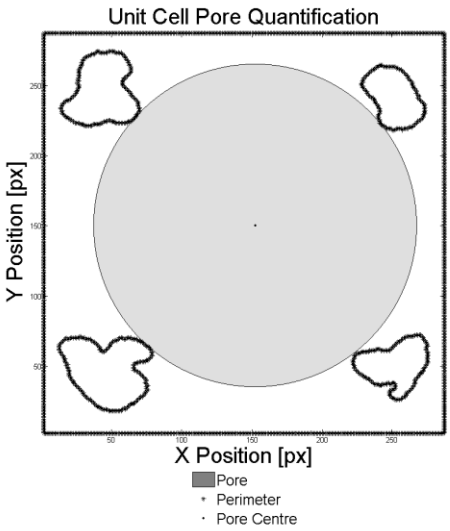

Fig. 9. Two dimensional pore quantification of the pore in the simple cubic scaffold unit cell shown in Fig. 7 The pore diameter was determined to be 3.39 mm based on a scan resolution of 17.47 µm/px.

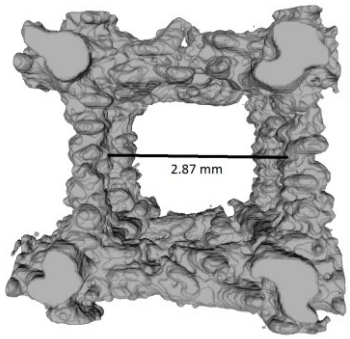

Fig. 10. Pore size measurement from µCT reconstruction showing the pore diameter measurement that would be reported using a traditional method. The pore diameter was determined to be 2.87 mm.

Table 2. Pore measurements of a simple scaffold

Spherical Pore Approximation Model	Traditional measurement of pore diameter	Difference
3.39 mm	2.87 mm	-15%

The measured pore diameters in Table 2 indicate that a traditional reporting technique gives a smaller pore diameter than the spherical pore approximation model measuring the pore diameter within the scaffold cell. Furthermore, according to the spherical pore approximation model, the measurement of the distance between struts at the surface of a scaffold would more accurately describe the diameter of an interconnecting region between fully contained pores.

3.3 A complex pore in two dimensions

A two dimensional slice of a complex scaffold was chosen and the pore size of a single pore was quantified. The pore located in the central region of the image was chosen for analysis. The original scaffold was cylindrical and nominally 5mm in diameter. The scan was performed at a resolution of 6.94 µm/px.\

Fig. 11. The filtered and thresholded central region of a two dimensional slice reconstructed from a µCT scan of a complex EBM scaffold.

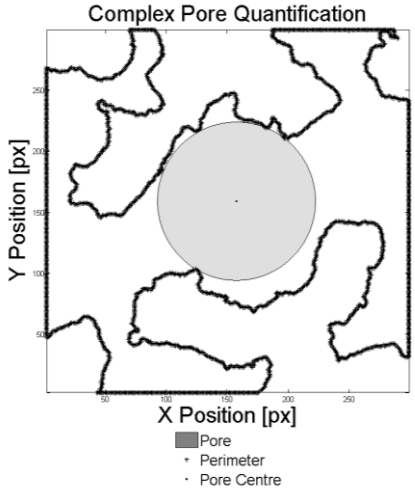

Fig. 12. The processed image showing the pore quantified.

Table 3. Complex pore quantification

Measured Pore Diameter [px]	Measured Pore Diameter [µm]
129.4	898.0

From an arbitrary starting location in the central region of the image a pore was successfully located. The pore migration allowed for the maximisation of the pore within the area of interest. The maximum diameter of a circular pore in this region was found to be 898.0 µm.

This evaluation was performed at the full resolution of the original data (300x300 px). A comparison was made between full resolution data and half resolution data to show that search time can be reduced by down sampling the data with negligible effect on the accuracy of the results. A 75% reduction in the number of pixels in the image resulted in the computation time dropping to 50% of the original value with an insignificant 0.1% change in the diameter of the pore.

Table 4. Effect of resolution on computation time

Particular	Value		Difference
Image size [px]	300x300	150x150	-75%
Time [sec]	0.021	0.011	-50%
Pore dia [µm]	898.0	897.2	-0.1%

4. DISCUSSION AND FUTURE WORK

The pore model and quantification algorithm was successfully implemented for a phantom scaffold and simple and complex EBM scaffolds in two dimensions only. A three dimensional implementation of the algorithm would allow this method to be used for the volumetric quantification of pore size from µCT data.

The pore model was effective for approximating complex pore architecture. The pore centre migration methods were found to be effective in discovering the local maxima in pore diameter within the complex topography of EBM scaffolds.

In the two dimensional analysis of a phantom scaffold the algorithm determined the pore size to within 2.7% of the actual maximum diameter of the region of interest. The spherical pore approximation model reported a larger pore diameter than a traditional µCT technique. For high resolution data it was shown that a pore can be effectively and quickly discovered and that the computation time can be decreased significantly by down sampling the data with little loss of accuracy.

5. REFERENCES

Alvarez, K., Nakajima, H. (2009). Metallic scaffolds for bone regeneration, *Materials 2*, Issue 3, Pages 790-832.

Ho, S.T., Hutmacher, D.W. (2006). A comparison of micro CT with other techniques used in the characterization of scaffolds, *Biomaterials,* Volume 27, Issue 8, Pages 1362-1376.

Jones, A., et al. (2004). Analysis of 3D bone ingrowth into polymer scaffolds via micro-computed tomography imaging, *Biomaterials*, Volume 25, Issue 20, Pages 4947-4954.

Karageorgiou, V., Kaplan, D. (2005). Porosity of 3D biomaterial scaffolds and osseogenesis, *Biomaterials,* Volume 26, Issue 27, Pages 5474-5491.

Marin, E., et al. (2010) Characterization of cellular solids in Ti6Al4V for Orthopaedic implant applications: Trabecular titanium, *Journal of the Mechanical Behaviour of Biomedical Materials 3,* Issue 5, Pages 373-381.

Pedoe, D. (1995). *Circles: A Mathematical View*, rev. ed. Washington, DC: Math. Assoc. Amer.